

FRAGILE DYNAMICS ENABLE DIVERSE GENOMIC DETERMINANTS TO INFLUENCE ARRHYTHMIA PROPENSITY

Authors: Tim J Kamerzell^{1,2,3}, Eric A Sobie¹, Kai-Chen Yang^{2,‡}, Jeanne M Nerbonne², Calum A MacRae³ and Ravi Iyengar^{1*}

Affiliations:

¹Department of Pharmacology and Systems Therapeutics and Systems Biology Center New York, Icahn School of Medicine at Mount Sinai, New York City, NY, USA.

²Department of Developmental Biology and Center for Cardiovascular Research, Division of Cardiology, Department of Internal Medicine, Washington University School of Medicine, Saint Louis, MO, USA.

³Brigham and Women's Hospital, Cardiovascular Division, Boston, MA, USA and Harvard Medical School, Boston, MA, USA.

*Correspondence to: Ravi Iyengar. Department of Pharmacology and Systems Therapeutics and Systems Biology Center New York, Icahn School of Medicine at Mount Sinai, New York City, NY 10029. Email: ravi.iyengar@mssm.edu.

‡ Current address: Department of Pharmacology, National Taiwan University School of Medicine, Taipei, Taiwan.

Abstract:

Genotype-phenotype relationships are determinants of human diseases. Often, we know little about why so many genes are involved in complex common diseases. We hypothesized that this multigene effect arises from the relationship between genes and physiological dynamics. We tested this hypothesis for arrhythmias as physiological dynamics define this disease. We integrated graph theory analysis of genomic and protein-protein interaction networks with dynamical models of ion channel function to identify the physiological dynamics of genome wide variation for five different arrhythmias. Regulatory networks for the cardiac conduction system and arrhythmias were constructed from GWAS and known disease genes. Electrophysiological models of myocyte action potentials were used to conduct extensive parameter variations to identify robust and fragile kinetic parameters that were then, using regulatory networks, associated with genomic determinants. We find that genome-wide determinants of arrhythmias that represent many cellular processes are selectively associated with fragile physiological dynamics of ion channel kinetics. This association predicts disease propensity. Deep RNA sequencing from human left ventricular tissue of arrhythmia and control subjects confirmed the predictive relationship. Taken together these studies show that the varied multigene effects of arrhythmias arises because of associations with fragile kinetic parameters of cardiac electrophysiology.

Significance Statement:

Our understanding of the genetics of common diseases has advanced exponentially over the past decade. We now know that differences and variation in multiple genes contribute to disease susceptibility with significant heterogeneity in the phenotype. However, how genetic variation contributes to disease phenotypes remains unknown. We hypothesized that the relationships between physiological dynamics and genetic architecture is a fundamental determinant of disease susceptibility and genetic heterogeneity. To test our hypothesis, we integrated mathematical models of cardiac electrophysiology with genetic network models of cardiac arrhythmias. We found that disease related genome variants were selectively associated with fragile kinetic parameters that predict disease propensity and identified several novel cellular processes associated with arrhythmogenesis.

43 INTRODUCTION

44 The genetic architecture of many common diseases has been extensively studied over the past decade providing
45 valuable insight into the etiology of disease (1, 2). Differences and variation in genetic architecture contribute to
46 disease susceptibility (1-4). Despite tremendous advances in the genetic basis of these diseases our
47 understanding of how and why genomic changes manifest as disease phenotype remains incomplete and our
48 ability to predict disease risk is often inadequate. This is especially true for many complex progressive diseases
49 including autoimmune disorders, neuropsychiatric diseases, diabetes and cardiovascular diseases. The
50 relationships between genotype and phenotype are complex because they are based on genetic heterogeneity,
51 the environment and the dynamics of physiology resulting in nonlinear interactions between genes and gene
52 products (1, 2, 5-7). We sought to identify a simple principle as to why so many varied genomic determinants
53 are involved in disease phenotype. We hypothesized that the involvement could be due to a selective association
54 with fragile features of the physiological dynamics. To test this hypothesis we used a model integration
55 approach combining network models with multi-compartment ODE models.

56 Arrhythmias are complex diseases that most often arise from mutations in genes that encode ion
57 channels ultimately leading to altered physiological dynamics. Nevertheless, recent evidence suggests that
58 drivers of conduction abnormalities and arrhythmias can extend well beyond mutated channel proteins. For
59 example, *Wnt11* has been associated with the ECG PR interval in GWAS (8) and in a separate study was shown
60 to pattern a myocardial electrical gradient through regulation of the L-type Ca^{2+} channel (9). Similarly, the
61 transcription factor *PITX2*, has been associated with atrial fibrillation in GWAS (10) and was subsequently
62 shown to regulate ion transport and impair calcium handling (11, 12). A multi-model approach that integrates
63 physiological dynamics, cell regulatory networks and genetic architecture could provide insight as to why such
64 varied genes are involved. Using canonical cell biological knowledge it is possible to schematically describe the
65 relationships between cell regulatory networks to cardiac myocyte action potentials and consequently to
66 conduction abnormalities. To mechanistically connect genomic variations to physiological dynamics we need to
67 integrate two types of computational models: (1) network models that delineate the topology of regulation in
68 terms of gene products (proteins) and their interactions and (2) dynamical models that describe the time course
69 of physiological responses (i.e. ion channel function) in terms of protein function. Both types of models have
70 been used to study arrhythmias. Previous network analysis studies have shown considerable overlap in the
71 human interactome between products of genes that can cause Long QT syndrome when mutated and targets of
72 drugs that can cause adverse cardiac events (13, 14). This analysis generated the prediction, subsequently
73 validated by clinical observations, that loperamide could cause arrhythmias (15). A different computational
74 approach, combining statistical regression analysis with dynamical models of cardiac electrophysiology, at the

cellular and organ levels, also provided deep insight into the quantitative dynamic relationship between the cardiomyocyte action potential and the heart's electrical activity (16). Systematic parameter sensitivity analysis of cardiomyocyte models generate precise predictions of how alterations in any cardiac ionic current may either exacerbate or mitigate pathological alterations to the electrocardiogram (16-20). This approach can quantitatively classify electrophysiological parameters as either fragile, meaning that small changes in parameters can cause large physiological alterations, or robust, meaning that cells or tissues can tolerate large changes to the parameter values without altering physiological responses.

To test our hypothesis that disease related genes might associate with the fragile features of physiological dynamics we integrated the network and dynamical models. We found that disease related genome variants were selectively associated with fragile kinetic parameters. Model integration also identified several cellular processes that could be associated with arrhythmogenesis. Using deep RNA sequencing data from human cardiac tissue from patients with arrhythmias we verified many key predictions from our integrated model including an association of arrhythmias with fragile kinetic parameters and the involvement of pathways such as propanoate metabolism. We combined multiscale data with unsupervised learning to identify genomic determinants of disease that correlate with fragile genes allowing us to demonstrate why genes belonging to many cellular processes are associated with increased disease propensity.

RESULTS

We studied the systems biology of arrhythmias through integration of graph theory and dynamical modeling, combined with transcriptomic analysis of human heart tissue, to better understand how genomic architecture can contribute to cardiac electrical phenotypes. **Figure 1** shows a schematic of the computational and experimental methods used in this study. Initially, we compiled prior information from classical disease gene discovery and GWA studies to comprehensively catalog genomic determinants, including mutations, SNPs and other genomic variants, known to be associated with ECG characteristics and five types of arrhythmias. This database of genes was then used to build protein-protein interaction networks and identify potential novel disease mechanisms. Next, we used well known ordinary differential equation based models of the cardiomyocyte action potential to identify parameters (kinetic properties of gene products) that were either sensitive (fragile) or robust to modulation. Our approach surprisingly identified that fragile kinetic parameters are preferentially associated with disease related genomic determinants. The network analysis also generated the unexpected prediction that arrhythmia genes are closely associated with genes involved in previously unrelated cellular processes, including propanoate metabolism, the ubiquitin proteasomal degradation pathway, and

106 histone modification and chromatin remodeling. We then validated numerous predictions from our models
107 using transcriptomic profiling of human left ventricular tissue from patients with arrhythmias.

109 **Networks from ECG and arrhythmia genomic determinants identify new biological associations**

110 We utilized published human studies to identify all known genes associated both with the ECG and five
111 different arrhythmias: atrial fibrillation, QT-Opathies, Brugada, catecholaminergic polymorphic ventricular
112 tachycardia (CPVT) and progressive cardiac conduction defect (PCCD) (**Supplementary Fig. 1a-b**). We
113 identified relevant genes from classical disease gene discovery studies and mapped or reported genes from
114 SNPs identified in genome wide association studies (GWAS). The full list of seed genes (153 for ECG and 109
115 for arrhythmia networks) is provided in **Supplementary Tables 1-2**. Often the same gene/gene-products are
116 involved in multiples phases of the ECG or different types of arrhythmias. These relationships are shown in
117 **Supplementary Figures 1c-e**. Individual genes may contribute to multiple electrophysiological responses
118 (pleiotropy) and multiple genes can affect individual phenotypes (epistasis) (21, 22). Examples include,
119 SCN5A, the gene encoding for the cardiac voltage-gated sodium channel, associated with several ECG
120 characteristics (PR interval, QRS duration and QT interval) and arrhythmias (atrial fibrillation, QT-opathies,
121 Brugada syndrome and PCCD) (8, 21, 23-25), and cardiac transcription factors such as NKX2-5, SOX5, and
122 TBX5. Many of the genes are known ion channels or channel associated membrane proteins, but other known
123 functions include cardiovascular development and intracellular signaling. The overlap of individual ECG and
124 arrhythmia network genes is shown as Venn diagrams in **Supplementary Figure 2**.

125 Using genes associated with particular arrhythmias and ECG characteristics as seed nodes, we
126 developed biological interaction networks by expanding around these nodes using protein-protein interactions
127 (26, 27). Networks were constructed using direct protein interactions with seed genes and one intermediate node
128 to connect the seed nodes. In the Supplementary Materials Section we describe the databases from which
129 human protein interactions were imported and the methods used to expand ECG and arrhythmia network genes
130 to 4190 and 4955 components, respectively. Representative networks for five separate arrhythmias and
131 components of the ECG are shown in **Supplementary Figure 3**.

132 Atrial fibrillation is the most common human cardiac arrhythmia with a rapidly increasing prevalence
133 and incidence worldwide. The atrial fibrillation network is shown in **Figure 2a** with several highlighted clusters
134 of densely connected nodes identified based on connectedness and biological function. For example, the cluster
135 of red nodes (genes) in the top right corner of Figure 2 is enriched for genes involved in propanoate metabolism.

136 Functional gene enrichment of each arrhythmia network was used to identify biological processes potentially
137 contributing to disease. Overrepresented gene ontology terms were determined from lists of genes that make up
138 each network (28). **Figure 2b** shows a functional enrichment network of the most significant biological
139 processes involved with atrial fibrillation. Nodes in the enrichment network indicate the most over-represented
140 biological processes, with node size scaled using the betweenness centrality and color coded according to the
141 biological process (metabolism, histone modification, etc.). Edges between nodes, with thickness scaled using
142 edge betweenness, indicate that multiple genes contribute to each process. For example, genes within the atrial
143 fibrillation network that are involved with Wnt signaling also contribute to heart development, chromatin
144 modification and androgen signaling, among others. **Supplementary Table 3** summarizes the most significant
145 enrichment terms used to describe the set of network genes for all five arrhythmias.

146 The biological functions of genes contributing to the arrhythmia networks can be classified into seven
147 major groups; cellular signaling, transport (including ion channels), metabolism, protein turnover, gene
148 expression, chromatin and histone modifications, and development. The similarities and differences between
149 arrhythmia networks were identified and categorized for each of the seven major groupings (**Supplementary**
150 **Table 3**). Significant overlap of enriched biological processes from genes involved with arrhythmias was found.
151 This analysis revealed several cellular processes that have not been previously associated with
152 arrhythmogenesis. For example, RNA splicing, ubiquitin degradation, membrane transport and metabolism,
153 more specifically propanoate metabolism, were all enriched in multiple arrhythmia networks. The network
154 models therefore generate potentially testable hypotheses by suggesting that these biological processes may be
155 related to the pathophysiology of arrhythmias. Although the expanded networks most certainly contain some
156 genes that do not contribute to disease it is less likely that these “non-disease” genes will be identified as highly
157 enriched or components of highly connected dense clusters. Furthermore, we verified many of the biological
158 processes identified in the networks using human RNA sequencing and functional knockdown experiments in
159 zebrafish.

160 The macro-scale topology of arrhythmia networks shows well-connected communities linked to more
161 isolated communities. Each network is defined by a number of dense communities or hubs connected to other
162 regions of the network via less well connected or sparse clusters. The Venn diagrams readily highlight the
163 substantial genetic overlap and number of unique genes between the various ECG and arrhythmia components
164 suggesting a large number of potential disease or modifier genes involved with the cardiac electrical response
165 including the diversity of molecular responses leading to phenotypic heterogeneity. That is, there are many
166 different routes to disease. To further characterize network structure we calculated topological parameters and
167 various network statistics (**Supplementary Figures 4-13**). Both the ECG and arrhythmia networks are

168 approximately scale free with power law like degree distributions (**Supplementary Figures 4 and 6**). The
169 degree distributions of these real world genetic interaction ECG and arrhythmia networks systematically and
170 expectedly deviate from the degree distributions of random networks with the same number of nodes and edges
171 (**Supplementary Figures 5 and 7**). To assess global (average) network metrics, we calculated the average
172 clustering coefficient, density, heterogeneity, centralization and characteristic path length of each network
173 (**Supplementary Figures 8 and 9**) (29). The network statistics confirmed the visual impression that these
174 networks are highly connected, dense and heterogeneous with high degrees of centrality measures as compared
175 to random networks. These findings are expected and suggest that arrhythmia networks comprise a large
176 number of essential disease genes or modifier disease genes with potentially fragile interdependencies (30-32).

178 **Deep RNA sequencing of human subjects with arrhythmias confirms association of new cellular** 179 **processes with disease**

180 We used deep RNA sequencing of human subjects with arrhythmias to independently confirm the novel
181 cellular processes associated with arrhythmias that were separately identified from enrichment analysis of the
182 biological interaction networks. The ventricular myocardial transcriptional profiles of human subjects with
183 arrhythmias were analyzed and compared with those of human subjects without disease (**Figure 3**). Genes with
184 the largest difference in expression were statistically analyzed for significance and those with statistically
185 significant differences ($p \leq 0.05$) were included in gene enrichment analysis. The Fisher exact test with
186 associated p-values was used for enrichment analysis in the program Enrichr (28). Many of the same biological
187 processes identified from enrichment analysis of the biological network models were also identified using
188 enrichment analysis of the genes from human RNA sequencing. Representative heat maps of differences in
189 expression profiles involved with propanoate metabolism (**Fig. 3a**) and membrane transport, RNA splicing and
190 cardiovascular development (**Fig. 3b**) highlight some of the changes in the respective cellular processes
191 enriched in human subjects with arrhythmias. These findings confirm the identification of novel cellular
192 processes associated with arrhythmias. In addition to identifying new cellular processes, previously known
193 mechanisms of arrhythmogenesis were also confirmed. A comparison of overlapping gene enrichment terms
194 identified using network analysis and human RNA sequencing is shown in **Figures 3c-d** highlighting many new
195 and well known biological processes. In fact, the overlap of all human RNA seq enrichment terms with the
196 atrial fibrillation network enrichment terms is nearly 70% and greater than 50% overlap is observed with all
197 other arrhythmia networks (**Fig. 3d**).

199 **From topology to dynamics: Mapping the kinetic parameters that contribute to the fragility of dynamics** 200 **onto genes**

201 The topological network and enrichment analyses are useful in understanding at a global level the subcellular
202 processes involved in arrhythmias, however, network models do not provide information about physiological
203 dynamics. Hence we sought to integrate dynamical models of cardiac electrophysiology with the gene
204 interaction network models. This integrated computational analysis can help us ascertain the value of genomic
205 changes in altering physiological responses. The dynamical models identify both fragile and robust genes
206 potentially contributing to disease which may also be useful for predicting disease propensity.

207 Using well-established dynamical models, we conducted massive simulations of atrial, ventricular and
208 SA node cardiac action potentials by systematically varying the parameters that define the conductances and
209 rates of ion transport (16, 18, 33-36). **Figures 4a-c** show representative voltage, intracellular calcium and
210 subspace calcium tracings from a single simulation of the ventricular action potential. **Figures 4d-f** shows many
211 ventricular, atrial and SA node action potential tracings from massive simulations while varying the model
212 parameters that define ionic conductances. Changing kinetic parameters differentially modulates the voltage
213 tracings. Some kinetic parameters substantially influence the voltage tracings while others only modestly
214 perturb voltage. These simulations allowed us to quantify how sensitive the different action potential models are
215 to changes in the various ionic conductances which can then be linked to genes.

216 Multivariate regression and failure score analysis were used to quantify the sensitivity of the action
217 potential duration and calcium transients to changes in individual and pairwise parameters (**Figures 4g-h and**
218 **Supplementary Figures 14-15**). To perform pairwise parameter analysis we simultaneously varied two
219 parameters while recording the outputs at the end of the simulation. The magnitude of the regression
220 coefficients from regression analysis are quantitative measures of the sensitivity of simulation outputs (e.g.,
221 voltage, calcium transients) to parameter perturbation (e.g., varying L-type Ca^{2+} conductance). We also
222 calculated a catastrophic failure score that represents the relative likelihood of a failed action potential due to
223 changes in kinetic parameters (ionic conductances). **Figures 4g-h** show the calculated failure scores for
224 ventricular and SA node models while varying each parameter. The failure scores and regression coefficients
225 (parameter sensitivities) represent quantitative dynamic measures of the cardiac electrophysiological response
226 to perturbation. We defined fragile parameters as those that contribute to nearly 80% of the failures of action
227 potential propagation upon perturbation. Thus the molecular kinetic parameters most sensitive to perturbation
228 are more fragile at a whole cell and organ level as these parameters are more likely to contribute to action
229 potential failure and arrhythmogenesis when perturbed even by a small amount.

Our analysis shows that the cardiac action potential is most sensitive to perturbations in the L-type Ca^{2+} current (G_{CaL}), Na^+ - Ca^{2+} exchange current (kNaCa, NCX), and rapid delayed rectifier K^+ current (G_{Kr}). The Na^+ current, Na^+ - K^+ pump current (I_{NaK}) and the cardiac ryanodine receptor channels (RyR) current are also sensitive parameters. The relative importance of each parameter varies according to the model used (SA node, ventricular or atrial AP); however, nearly 80% of the failure scores can be accounted for by sensitivity to perturbation in the aforementioned parameters. Multiparameter sensitivity analysis thus provides a quantitative measure of simultaneous electrophysiological perturbation that can be connected phenomenologically to genes comprising arrhythmia networks and used to help explain phenotypic variation.

To determine the relationship between genomic characteristics to electrophysiological dynamics and phenotypes we mapped genes identified in the networks to the sensitive model parameters. Network genes were associated with the dynamical model parameters based on function of the gene and parameter. **Supplementary Figure 16** lists some of the important associations between dynamical parameters and network genes. We refer to the nodes that map to the most sensitive parameters as fragile genes – those that, when altered, might result in a greater propensity for developing arrhythmias. An additional network was then constructed connecting dynamical model parameters to genes with the node size scaled to represent parameter fragility and genetic variation obtained from the NCBI databases and Variation Viewer (**Fig. 4i**). For example, the Na^+ - Ca^{2+} exchange current, which directly maps to the network node SLC8A1, was shown to be a sensitive parameter from the action potential simulations. Similarly, KCNQ1 and KCNE1, known potassium voltage-gated channel genes required for repolarization, directly map to the slow delayed rectifier K^+ current parameter, G_{Ks} .

Human RNA sequencing supports the association of genes with fragile dynamics with arrhythmias

Having computationally identified that specific genes involved with arrhythmias have fragile dynamics we sought to test if this computational prediction could be experimentally validated. Fragile dynamics means sensitivity to perturbation and can arise both from variation in kinetic parameters and levels of the reactants. Assuming that mRNA levels could overall reflect protein levels we formulated the hypothesis that fragile genes would show greater changes in disease state or would result in greater changes in other protein levels as a compensatory change. This is in fact how we define sensitive parameters in our dynamical model. Therefore, using human RNA sequencing as our experimental approach and genomic analysis, we sought to determine if this association was valid and identify new mechanisms potentially contributing to disease. In these analyses we also sought to determine the characteristics and potential mechanisms underlying this association.

We evaluated human ventricular tissue gene expression profiles of the genes computationally identified to have fragile dynamics in subjects with and without arrhythmias (**Figure 4j**). The methods used for RNA sequencing have been previously described (21) and in the Supplementary Materials section. **Figure 4j** shows the difference in expression of select fragile genes (as a heat map) between subjects with and without arrhythmias, highlighting the substantial changes when a perturbation (human subjects with arrhythmias) is introduced. The Na⁺-K⁺ ATPase gene has the highest failure score based on the computational ventricular model and also shows one of the highest changes in gene expression in human ventricular tissue in arrhythmia patients. There are considerable differences in expression levels of many genes with fragile dynamics. This data supports our hypothesis that genes with fragile dynamics are likely to show greater changes in their tissue level expression in the disease state.

We also used the human RNA expression profiles to further support the association of fragile dynamics with arrhythmia genes by calculating *in-vivo* robustness and fragility of genes using previously described methods based on variational principles (37). When using human RNA sequencing, fragility can be defined as large changes in gene expression variation in the presence of perturbation (arrhythmogenesis) and/or the change in variance of gene expression between subjects with and without arrhythmias. The variance of robust genes is predicted not to change a significant amount between control subjects and those with disease. If both control and disease gene expression levels are highly variable then the change in variance will be small. Similarly, if the variance of both control and disease gene expression levels is small then the change in variance will be small. In contrast, if the variance of control genes is small but the variance of disease genes is large (vice versa) then the change in variance will be large. That is, fragile genes may show large changes in variance upon perturbation suggesting sensitivity to changes in disease state.

Figure 4k shows the change in gene expression variance between human subjects with arrhythmias and subjects without arrhythmias for nearly 20,000 different genes. The 90th percentile of change in variance values are between the two dashed blue lines outlined in the figure. That is most genes are characterized by relatively small changes in variance. These genes with low change in variance can be considered robust genes as previously described (37). The red dashed line denotes the median value of change in variance for all 20,000 genes. The change in variance, of all genes with previously determined fragile dynamics by our computational methods, is greater than the 90th percentile and most values are greater than the 95th percentile suggesting these genes whose proteins have fragile dynamics are highly sensitive to changes in the disease state. The change in variance of three propanoate metabolism genes (HADHB, LDHA and LDHB) and four genes involved in calcium regulation and current (KCNIP2, ATP2A2, PLN and CASQ2) have values greater than the 99th

percentile. Therefore, human RNA sequencing of subjects with and without arrhythmias independently provides strong support for the computational finding associating fragile genes with disease.

Unsupervised learning identifies correlation between genomic architecture and fragile genes in subjects with arrhythmias

We next tested whether different types of genomic variations selectively contribute to the fragile dynamics of disease genes and provide additional mechanistic insight contributing to the likelihood of developing disease. To identify the genomic characteristics contributing to the fragility of the products of arrhythmia genes, we utilized two unsupervised learning methods, Self-Organizing Maps (SOMs) and Principal Component Analysis (PCA), to identify and classify the genomic differences (SNPs, CNVs, CpG counts, etc.) between clusters of fragile and robust genes comprising arrhythmia networks (**Figure 5 and supplementary Figure 17-18**). SOMs are dynamical, adaptive, nondeterministic and nonlinear, and can help to identify emergent properties. We trained the SOMs using diverse genomic characteristics (SNPs, CNVs, CpG counts, etc.) of the arrhythmia networks (**Supplementary Table 4**). **Figure 5a** shows a heat map of genomic characteristics for individual genes used to train the SOMs. A cluster of genes (cluster of red signatures) in the lower half of the heat map identifies many of the fragile seed nodes. This cluster is the same set of fragile genes identified using dynamical computational analysis and RNA sequencing. **Figure 5b** shows the SOM distance matrix, a representation that allows for visualization of the high-dimensional spaces defined by the genes and their characteristics. The map is organized into clusters of similar color and topological space. Individual red lines connect neighboring nodes of the SOM and the colors in the regions containing the red lines indicate the distances between nodes with lighter colors representing shorter distances. **Supplementary Figure 18** shows the PCA plot as projections of the data set to the subspace spanned by the two eigenvectors with greatest eigenvalues. Individual component planes and U-matrices identify clusters of genes and the PCA projections associate the features that contribute most to the gene clusters. **Figure 5c** shows the number of genes associated with each cluster with the fragile gene cluster outlined. Fragile genes were most dissimilar to the other genes (robust genes) and form their own cluster. The SOMs, therefore, efficiently separate clusters of fragile and robust genes based on their genomic characteristics (SNPs, CNVs, CpG counts, etc.). Fragile gene clusters are most closely associated with increased frequency of SNPs, indels, simple repeats, DNase hypersensitivity sites and novel sequence insertions. We then evaluated the biological function of the most fragile genes that clustered together in the SOMs. The most fragile genes from SOM cluster analysis were multiple genes involved with

321 calcium handling and excitation-contraction coupling (RYR2, CACNA1C, TRDN, CACNA2D1), the rapid
322 delayed rectifier K⁺ current (KCNQ1, KCNH2) and Na⁺-Ca²⁺ exchange current (ANK2 and SLC8A1).

323 Partial least squares (PLS) regression analysis was used to construct a model that relates genomic
324 architecture and fragility to disease propensity. Disease propensity is the likelihood of developing an arrhythmia
325 based on the failure of propagating an action potential. The PLS model is an independent model that
326 incorporates quantitative information obtained from our dynamical analysis and genomic characteristics to
327 predict disease propensity. **Figure 5d** shows the relationship between the fragile indices of seed node genes and
328 their disease propensity with the best fit linear surface response shown as a plane ($R^2 = 0.96$). The x and y axes,
329 labeled as fragile index 1 and 2, are the two scores from the PLS regression analysis which together capture
330 >85% of the variation contained in the 28 different genomic features. The z axis, labeled as disease propensity,
331 represents the failure scores for individual genes derived from the dynamical ODE simulations (**Figure 3g-h**).
332 **Figure 5e** shows the actual disease propensity score vs the fitted disease propensity score from our model ($R^2 =$
333 0.94) and confirms the three component PLSR model predicts the response well.

334 The SOMs identified and confirm novel fragile genes and the genetic architecture associated with
335 fragility. By looking at the biological function of fragile genes we gain insight to potential disease mechanisms.
336 For example, specific genes involved in metabolism, cellular signaling (e.g., Wnt, Notch, Ca²⁺), histone and
337 chromatin modification and regulation of RNA splicing also cluster with fragile channel genes. Several of our
338 novel pathway findings were also supported by the literature. For example, multiple clinical trials suggest that
339 histone deacetylase inhibitors and chromatin modulation influences cardiac electrical activity as seen by
340 increased frequency of QT interval prolongation, T wave flattening and atrial fibrillation (38). HDAC inhibition
341 also has been recently shown to reduce atrial fibrillation and remodeling in dogs (39).

342 We were particularly interested in a specific set of novel fragile genes involved in propanoate and
343 butanoate metabolism that were predicted to influence arrhythmogenesis. At least one study associated inborn
344 errors of metabolism caused by deficiency of propionyl CoA carboxylase with electrophysiological changes
345 including prolongation of the QT interval (40) and two cases report children with propionic acidemia leading to
346 arrhythmias with fatal outcomes (41, 42). Propanoate metabolism genes possess unique biological functions,
347 network metrics (avg. shortest path length) and also associate with the fragile genes using unsupervised learning
348 methods. Perhaps most importantly, the expression levels of propanoate metabolism genes were significantly
349 different in human subjects with arrhythmias compared to subjects without arrhythmias (**Figure 3a**). Their *in-*
350 *vivo* change in variance in human ventricular tissue also suggests that perturbation of their expression level may
351 contribute to disease (**Figure 4k**). These metabolic genes are crucial in amino acid, fatty acid and cholesterol

352 metabolism and many are expressed in the heart and muscle tissues (acetyl-CoA carboxylase), mitochondria
353 (propionyl-CoA carboxylase) and brain tissue, thus contributing to our interest in evaluating their possible link
354 to cardiac disease (43). In addition to the human RNA sequencing data that supports involvement of propanoate
355 metabolism in arrhythmias, we sought to further experimentally test the importance for cardiovascular function
356 using a series of zebrafish knockdown experiments. Morpholinos were used to knock down the propanoate
357 metabolism genes *SUCLG1/2*, *ACACA*, *PCCA* and *EHHADH* and cardiac phenotypes in zebrafish were
358 characterized using automated microscopic techniques. **Supplementary Figure 19** shows a combined box and
359 whiskers and scatter plots of zebrafish heart rates and cardiac output for wildtype and propanoate metabolism
360 gene knockdowns. Decreased contractility and morphologic changes in zebrafish hearts compared to wild type
361 were observed when individual propanoate metabolism genes were knocked down. An apparent decrease in
362 contractility was appreciated when *SUCLG1/2* and *ACACA* genes were knocked down while a more subtle yet
363 noteworthy change was also observed with *EHHADH*. Furthermore, quantitative decreases in heart rate and
364 cardiac output were measured when all gene products were altered. Representative images of wild type and
365 *ACACA* knockdown zebrafish hearts are shown in **supplementary figure 19**. Qualitatively, these images show
366 knockdowns with morphologically distinct hearts and increased pericardial edema indicative of impaired
367 cardiac activity.

369 **Discussion**

370 It is now widely accepted that most proteins function as components of networks, and considering their activity
371 in the context of the networks they belong to is useful for understanding how individual protein activities
372 contribute to network based emergent physiological functions. As a network node that is required for dynamic
373 function, a protein within a network needs to be defined by at least two characteristics, its quantity and its
374 ability to interact with its partners. These two characteristics are also the key parameters for the dynamical
375 models: initial concentration of reactant and reaction rate. Thus it should be relatively simple to convert a
376 directed sign-specified network into a system of coupled differential equations and thereby develop a systems
377 level understanding of why some genetic constructs but not others are correlated with disease phenotype.
378 However, our knowledge of protein concentrations and reaction rates is currently sparse, and it is not possible to
379 build reliable dynamical models directly from large network representations. New data integration methods are
380 needed to relate statistical and network representations to parameter values in dynamical models, and this study
381 represents a first step in that direction.

382 When starting the study we had thought that disease determinants would be associated with changes in
383 robust kinetics outside the boundaries of homeostatic tolerance and that these determinants would primarily be
384 coding variants. However, we found that specific types of both non-coding and coding variants in arrhythmia
385 genes were associated with fragile kinetics and correlate with disease propensity. Importantly, our studies show
386 that these multigene effects arise because of the association with fragile kinetic parameters of cardiac
387 electrophysiology. These results were unexpected, based on what is known for common cancer mechanisms
388 such as mutations in receptor tyrosine kinases and GTPases. We would have expected that robust kinetic
389 parameters of gene products could have been associated with overrepresented regions of structural variation in
390 the genome associated with arrhythmias. In fact, others have even suggested that because of evolutionary
391 selection constraints, it is just as likely that most genes involved in common polymorphic rearrangements are
392 tolerant of changes in certain types of architectural variation (44). The power obtained by integration of
393 multiple mathematical approaches and human RNA sequencing has enabled us to obtain a counterintuitive and
394 deep understanding of genotype-phenotype relationships and improved our ability to predict disease risk.

395 The data from multiple modeling studies, human RNA sequencing as well as the experiments in the
396 zebrafish model together support the hypothesis that the genetic architecture of fragile electrophysiological
397 responses and arrhythmias is responsible for increased disease propensity. The self-organizing maps efficiently
398 classify many genes as fragile and demonstrate substantial enrichment for genomic regions associated with
399 cardiac electrical parameters over the remainder of the genome. This is a new approach that provides a
400 comprehensive framework for understanding how variations of a convergent phenotype may manifest from
401 multigene interactions. Similar to other multigenic disorders that were initially characterized as being
402 monogenic, pathophysiologies of cardiac electrical activity are likely to be caused, modulated or suppressed by
403 allelic heterogeneity and mutations at multiple loci that are associated with fragile kinetics (45). Further
404 mechanistic understanding of how the multiple genomic loci interact will always come from studies focused on
405 physical and functional interactions or regulation of the proteins involved. This study provides direct evidence
406 in support of this assertion. It should be noted that the partial least square based correlation approach between
407 kinetic parameters and genomic loci has its limitation in providing comprehensive mechanistic understanding.
408 Nevertheless defining such relationships provides the boundary conditions within which the mechanisms will
409 operate.

410 The network based approach for prediction of additional genomic loci and testing of the predictions in
411 humans and the zebrafish models indicates that there are likely to be additional genomic loci that are related to
412 the origins of arrhythmias and disease progression or that contribute to disease propensity in the context of other
413 genomic variations or environmental effects. A collaborative study of Noonan syndrome allowed one of us to

414 use a pathway based approach to identify a gene that turned out to be disease related upon subsequent
415 laboratory based analyses of patient samples (46). Perhaps further studies on the genomes of patients with
416 arrhythmias could lead to the identification of additional genes involved in the pathophysiology of cardiac
417 electrophysiology and provide a basis for developing new drugs to treatment of arrhythmias. We suspect that
418 the novel relationships identified in this study between fragile kinetic parameters and architectural variation
419 could be a common theme for many diseases with common complex traits. For example, autism, schizophrenia,
420 epilepsy, Parkinson disease, Alzheimer disease, immunological disorders and emphysema, among others, have
421 all been shown to result from structural variation in the genomes of at least some patients (44). The challenge
422 will be to define kinetic parameters and identify models capable of recapitulating the relationship between
423 fragility in dynamics and genomic determinants as one cause in multiple complex diseases.

424
425
426
427
428
Acknowledgements: This research was supported by NIH grants P50-GM071558, R01-GM54508 and
429 R01-HL109264. TK was also supported by a fellowship from the Sarnoff Cardiovascular Research Foundation.
430
431
432
433
434
435
436
437
438

439 **Figure Legends**

440 **Figure 1. Schematic of methods used in this study**

441 (a) Networks of ECG components and arrhythmias were constructed from all known genes identified in genome
442 wide association studies (GWAS) and classical genetic approaches. Biological interaction networks identified
443 potential novel disease mechanisms. (b) Ordinary differential equation models of the cardiac action potential
444 were used to identify genes with sensitive changes to model parameters and subsequently mapped to genes
445 within the arrhythmia networks. (c) Human RNA sequencing verified several key predictions from the
446 arrhythmia network and ODE dynamic simulations. (d) Various unsupervised learning approaches were used to
447 identify genomic association with disease genes that predict disease propensity.

448 **Figure 2. The atrial fibrillation network**

449 (a) Representative atrial fibrillation interaction network. The nodes in each network represent a single protein or
450 gene and the edges connecting two nodes indicate an interaction. Clusters of highly interconnected nodes and
451 regions in the network are shown in color. Several clusters are magnified to highlight specific connections and
452 the associated genes within that cluster are labeled. Clusters of genes associated with propanoate metabolism
453 (red node cluster in top right corner), protein ubiquitination (blue node cluster), apoptosis and protein
454 processing (red node cluster in lower left corner) and cell-cell junctions and protein localization to the surface
455 (green node cluster) are shown.

456 (b) Functional gene enrichment network highlighting the most significant biological processes identified from
457 the atrial fibrillation arrhythmia network genes. Node size is scaled using the betweenness centrality and color
458 coded according to the associated biological process. Edges between nodes are scaled using edge betweenness
459 and indicate a significant number of genes contributing to the biological processes of both connected nodes. For
460 example, genes within the AF network involved with Wnt signaling are also involved with heart development,
461 chromatin modification, androgen receptor signaling, etc.

462 See **supplementary table 3** for a summary of various molecular processes associated with functional gene
463 enrichment of each arrhythmia network. The table is color coded by biological process to match the nodes and
464 network in figure 2D1.

465 **Figure 3. Human RNA sequencing reveals expression level differences and confirms biological processes associated with arrhythmias.**

466 Representative heat maps of gene expression level differences between human subjects with arrhythmias and
467 without arrhythmias. (a) Heat map of expression level differences in key propanoate metabolism genes. (b)
468 Heat map of expression level differences in key biological processes determined to be important by gene
469 enrichment analysis. (c) Table of highly ranked biological process terms using gene enrichment and gene
470 ontology. The table compares the top biological processes determined using network models and human RNA
471 sequencing data. The p-value is calculated using the Fisher exact test which is a proportion test that assumes a
472 binomial distribution and independence for probability of any gene belonging to any set. Gene enrichment
473 analysis and statistics were calculated using the Enrichr program previously described by Chen *et al* (28). (d)
474 Overlap of gene enrichment terms comparing network models to human RNA sequencing. The statistically
475 significant gene enrichment terms were identified from the genes in human RNA sequencing and separately for
476 each individual arrhythmia or ECG network. The number of terms that overlap were calculated as a percentage.
477 **ABBREVIATIONS:** ICM-ischemic cardiomyopathy; NICM-non ischemic cardiomyopathy; NF-control
478 subjects without arrhythmias or cardiomyopathy.

482 **Figure 4. Parameter sensitivity and failure analysis reveals fragile electrophysiological parameters that underlie arrhythmogenesis are also associated with disease genes from human RNA sequencing.**

483 Representative (a) voltage, (b) intracellular calcium and (c) subspace calcium tracings from a single simulation
484 of the ventricular cardiac action potential.

487 Many representative **(d)** ventricular, **(e)** atrial and **(f)** SA node action potential tracings from large scale
488 simulations while varying the models parameters. Dynamical model parameter failure scores, shown as bar
489 graphs, calculated from large scale simulations of the **(g)** ventricular and **(h)** atrial action potential. Failure
490 scores represent the sensitivity of the cardiac electrophysiological response to individual parameter variation.
491 Larger values of the failure score indicate a greater sensitivity to perturbation and an increased propensity for
492 arrhythmogenesis. For bar graphs of regression coefficients from parameter sensitivity analysis of large scale
493 simulations see **supplementary figures 14 and 15**.

494 **(i)** Fragile parameter-gene network showing the connection of key fragile genes to model parameters. Red
495 nodes indicate model parameters and blue nodes indicate linked genes. Node sizes are scaled to represent
496 electrophysiological parameter fragility and genetic variation. A list of model parameters and several associated
497 key fragile genes included in the gene networks listed with their corresponding failure scores is shown in
498 **supplementary figure 16**.

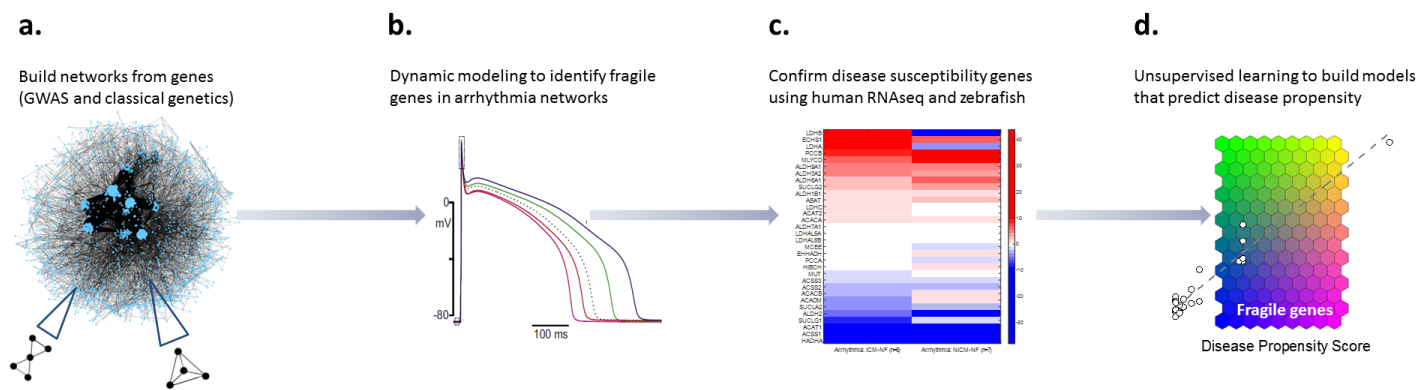
499 **(j)** Representative heat map of several fragile gene expression profiles of human subjects with arrhythmias. The
500 change in gene expression between human subjects with arrhythmias compared to control (subjects without
501 arrhythmias) are shown as red (positive) or blue (negative).

502 **(k)** Plot of the change in variance between human subjects with arrhythmias and control subjects for 20,000
503 different genes using human RNA sequencing data. The mean change in variance is shown as a dashed red line.
504 The 90th percentile of values are shown as dashed blue lines. All fragile genes lie above or below the dashed
505 blue lines.

506 **Figure 5. Variants in genes associated with fragile responses leads to disease**

507 Unsupervised learning was used to understand the complex genetic architecture of arrhythmias including the
508 sources of individual genetic variation that explain phenotypic variation. A density matrix was constructed
509 using 28 different genomic features to describe known arrhythmia genes (seed nodes from AF, QTopathies,
510 Brugada, CPVT and PCCD networks) and separately for each individual network gene. Genes were then
511 clustered based on similar genomic features using the self organizing map (SOM) approach. **(a)** Heat map of
512 normalized genomic feature values for all seed nodes based on the density matrix used to train the SOM. **(b)**
513 Self-organizing map unified distance matrix (U-matrix) constructed using genomic features of seed genes.
514 Individual red lines connect neighboring nodes (neural network) and the colors in the regions containing the red
515 lines indicate the distances between nodes (lighter colors shorter distances). The U-matrix provides a simple
516 way to visualize cluster boundaries on the map. **Supplementary figure 17** shows the individual weight matrix
517 SOMs for each of the features. **(c)** Self organizing topology map with the number of training data vectors
518 associated with each cluster. The fragile gene cluster is outlined in red. See **supplementary figure 18** for
519 principal component plots of the genes and features. **(d)** Three dimensional scatter plot of fragile seed gene
520 indices and their propensity for disease with best fit linear surface ($R^2 = 0.96$). Partial least squares regression
521 was used to construct a model using genomic features as an index of fragility and dynamical failure scores from
522 action potential simulations as propensity for disease. Three PLS components were used to explain > 90% of the
523 variation in genetic architecture. **(e)** Scatter plot of the observed disease propensity score and fitted disease
524 propensity score from the 3 component PLS model ($R^2 = 0.94$ for best linear fit).

533 **Figure 1.**



534

535

536

537

538

539

540

541

542

543

544

545

546

547

548

549

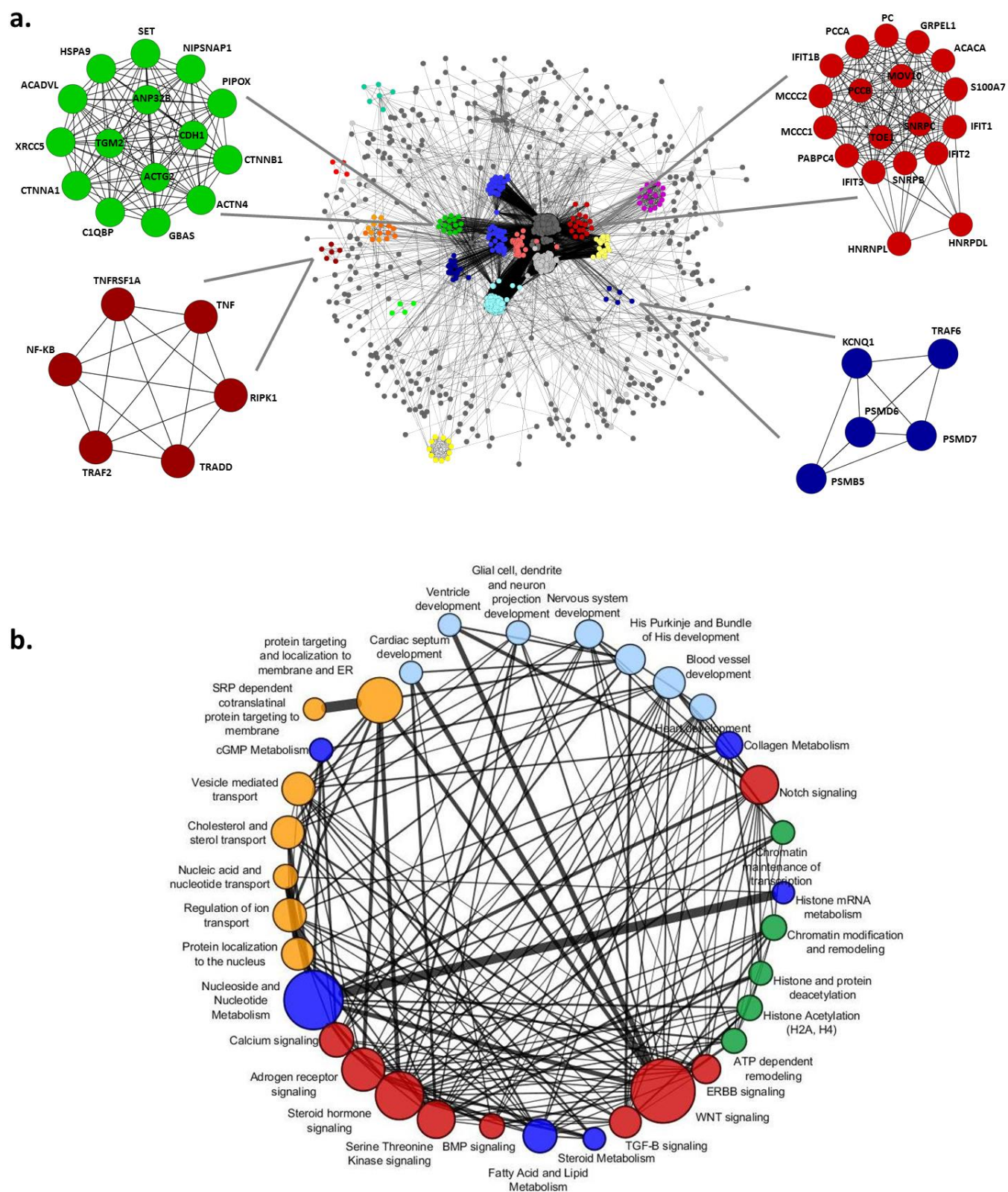
550

551

552

553

554 **Figure 2.**



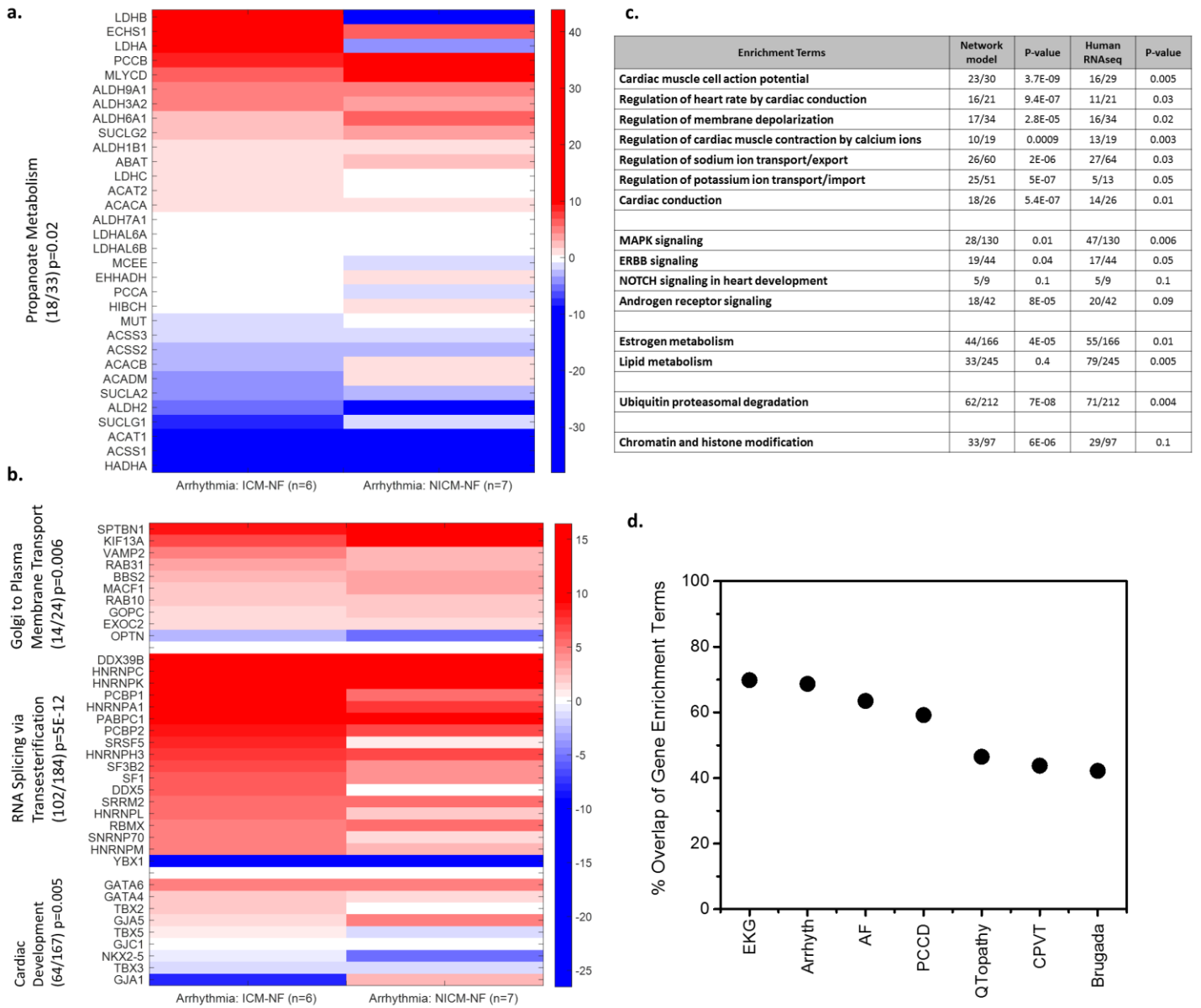
555

556

557

558

Figure 3.



559

560

561

562

563

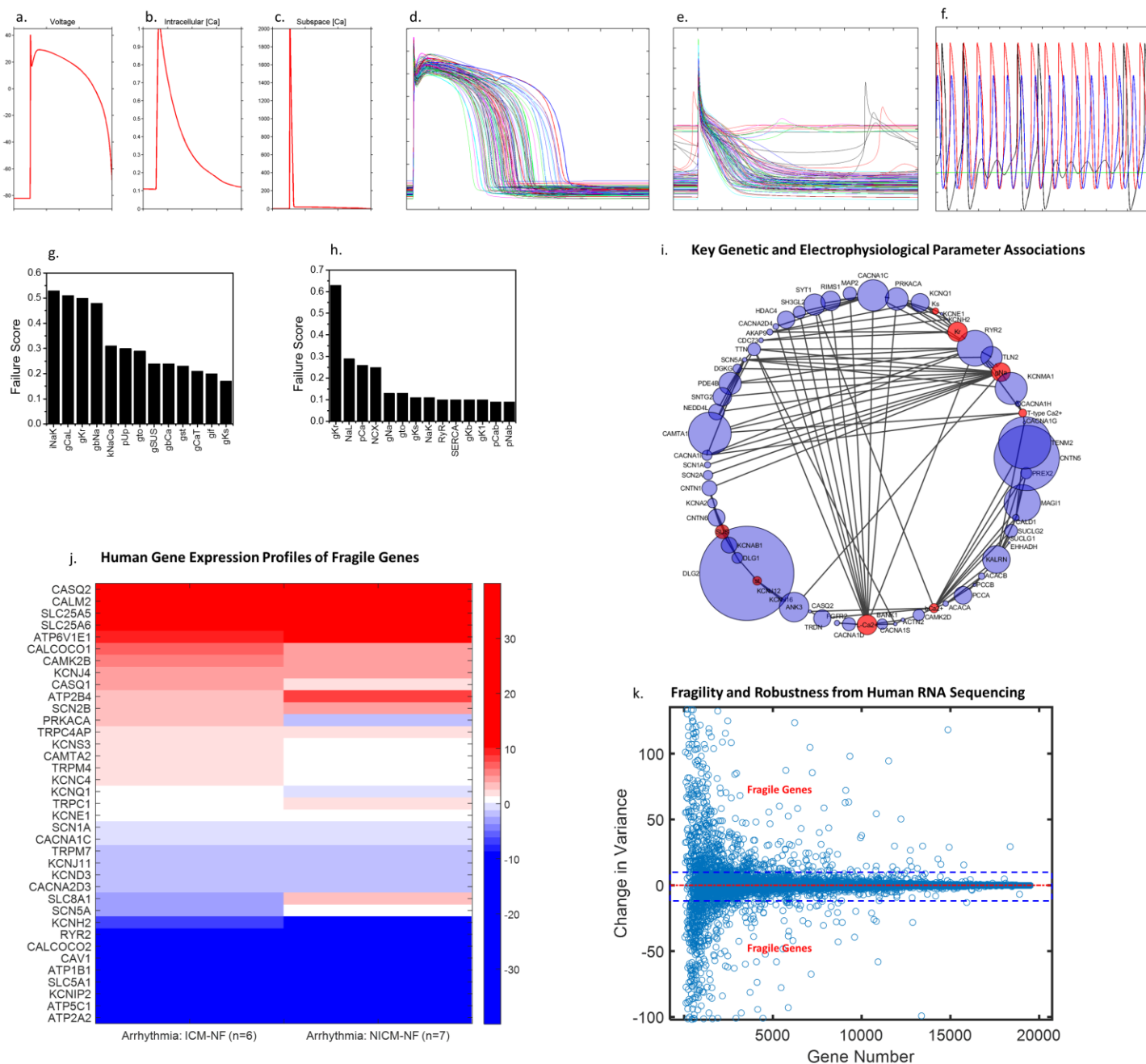
564

565

566

567

568 **Figure 4.**



569

570

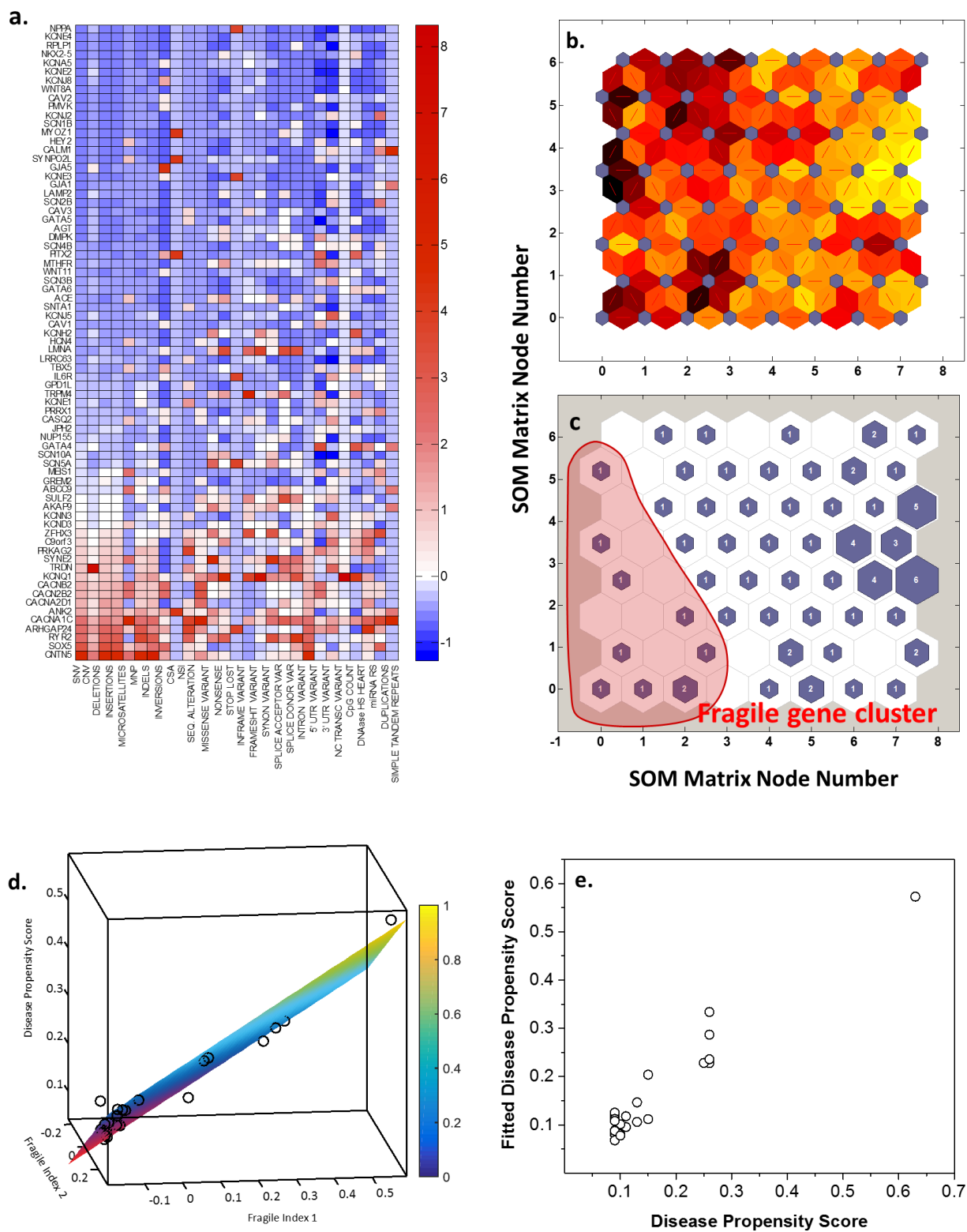
571

572

573

574

575 **Figure 5.**



576

577

578

References:

- 580 1. Albert FW & Kruglyak L (2015) The role of regulatory variation in complex traits and disease. *Nat Rev Genet* 16(4):197-
581 212.
- 582 2. Frazer KA, Murray SS, Schork NJ, & Topol EJ (2009) Human genetic variation and its contribution to complex traits. *Nat*
583 *Rev Genet* 10(4):241-251.
- 584 3. Feuk L, Carson AR, & Scherer SW (2006) Structural variation in the human genome. *Nat Rev Genet* 7(2):85-97.
- 585 4. Carvalho CM & Lupski JR (2016) Mechanisms underlying structural variant formation in genomic disorders. *Nat Rev Genet*
586 17(4):224-238.
- 587 5. Hoffmann AA, Sgro CM, & Lawler SH (1995) Ecological population genetics: the interface between genes and the
588 environment. *Annu Rev Genet* 29:349-370.
- 589 6. Lander ES & Schork NJ (1994) Genetic dissection of complex traits. *Science* 265(5181):2037-2048.
- 590 7. Lehner B (2013) Genotype to phenotype: lessons from model organisms for human genetics. *Nat Rev Genet* 14(3):168-178.
- 591 8. Pfeufer A, *et al.* (2010) Genome-wide association study of PR interval. *Nat Genet* 42(2):153-159.
- 592 9. Panakova D, Werdich AA, & Macrae CA (2010) Wnt11 patterns a myocardial electrical gradient through regulation of the L-
593 type Ca(2+) channel. *Nature* 466(7308):874-878.
- 594 10. Ellinor PT, *et al.* (2012) Meta-analysis identifies six new susceptibility loci for atrial fibrillation. *Nat Genet* 44(6):670-675.
- 595 11. Tao Y, *et al.* (2014) Pitx2, an atrial fibrillation predisposition gene, directly regulates ion transport and intercalated disc
596 genes. *Circ Cardiovasc Genet* 7(1):23-32.
- 597 12. Lozano-Velasco E, *et al.* (2016) Pitx2 impairs calcium handling in a dose-dependent manner by modulating Wnt signalling.
598 *Cardiovasc Res* 109(1):55-66.
- 599 13. Berger SI & Iyengar R (2011) Role of systems pharmacology in understanding drug adverse events. *Wiley Interdiscip Rev*
600 *Syst Biol Med* 3(2):129-135.
- 601 14. Berger SI, Ma'ayan A, & Iyengar R (2010) Systems pharmacology of arrhythmias. *Sci Signal* 3(118):ra30.
- 602 15. Marraffa JM, *et al.* (2014) Cardiac conduction disturbance after loperamide abuse. *Clin Toxicol (Phila)* 52(9):952-957.
- 603 16. Sobie EA (2009) Parameter sensitivity analysis in electrophysiological models using multivariable regression. *Biophys J*
604 96(4):1264-1274.
- 605 17. Sarkar AX, Christini DJ, & Sobie EA (2012) Exploiting mathematical models to illuminate electrophysiological variability
606 between individuals. *J Physiol* 590(Pt 11):2555-2567.
- 607 18. Sarkar AX & Sobie EA (2010) Regression analysis for constraining free parameters in electrophysiological models of cardiac
608 cells. *PLoS Comput Biol* 6(9):e1000914.
- 609 19. Sarkar AX & Sobie EA (2011) Quantification of repolarization reserve to understand interpatient variability in the response
610 to proarrhythmic drugs: a computational analysis. *Heart Rhythm* 8(11):1749-1755.
- 611 20. Sobie EA & Sarkar AX (2011) Regression methods for parameter sensitivity analysis: applications to cardiac arrhythmia
612 mechanisms. *Conf Proc IEEE Eng Med Biol Soc* 2011:4657-4660.
- 613 21. Milan DJ, Lubitz SA, Kaab S, & Ellinor PT (2010) Genome-wide association studies in cardiac electrophysiology: recent
614 discoveries and implications for clinical practice. *Heart Rhythm* 7(8):1141-1148.
- 615 22. Kolder IC, Tanck MW, & Bezzina CR (2012) Common genetic variation modulating cardiac ECG parameters and
616 susceptibility to sudden cardiac death. *J Mol Cell Cardiol* 52(3):620-629.
- 617 23. Holm H, *et al.* (2010) Several common variants modulate heart rate, PR interval and QRS duration. *Nat Genet* 42(2):117-
618 122.
- 619 24. Sotoodehnia N, *et al.* (2010) Common variants in 22 loci are associated with QRS duration and cardiac ventricular
620 conduction. *Nat Genet* 42(12):1068-1076.
- 621 25. Newton-Cheh C, *et al.* (2009) Common variants at ten loci influence QT interval duration in the QTGEN Study. *Nat Genet*
622 41(4):399-406.
- 623 26. Cerami EG, *et al.* (2011) Pathway Commons, a web resource for biological pathway data. *Nucleic acids research*
624 39(Database issue):D685-690.
- 625 27. Rolland T, *et al.* (2014) A proteome-scale map of the human interactome network. *Cell* 159(5):1212-1226.
- 626 28. Chen EY, *et al.* (2013) Enrichr: interactive and collaborative HTML5 gene list enrichment analysis tool. *BMC bioinformatics*
627 14:128.
- 628 29. Dong J & Horvath S (2007) Understanding network concepts in modules. *BMC Syst Biol* 1:24.
- 629 30. Barabasi AL, Gulbahce N, & Loscalzo J (2011) Network medicine: a network-based approach to human disease. *Nat Rev*
630 *Genet* 12(1):56-68.
- 631 31. Buldyrev SV, Parshani R, Paul G, Stanley HE, & Havlin S (2010) Catastrophic cascade of failures in interdependent
632 networks. *Nature* 464(7291):1025-1028.
- 633 32. Goh KI, *et al.* (2007) The human disease network. *Proc Natl Acad Sci U S A* 104(21):8685-8690.
- 634 33. Grandi E, *et al.* (2011) Human atrial action potential and Ca2+ model: sinus rhythm and chronic atrial fibrillation. *Circ Res*
635 109(9):1055-1066.

- 636 34. Maltsev VA & Lakatta EG (2009) Synergism of coupled subsarcolemmal Ca²⁺ clocks and sarcolemmal voltage clocks
637 confers robust and flexible pacemaker function in a novel pacemaker cell model. *Am J Physiol Heart Circ Physiol*
638 296(3):H594-615.
- 639 35. ten Tusscher KH, Noble D, Noble PJ, & Panfilov AV (2004) A model for human ventricular tissue. *Am J Physiol Heart Circ*
640 *Physiol* 286(4):H1573-1589.
- 641 36. O'Hara T, Virag L, Varro A, & Rudy Y (2011) Simulation of the undiseased human cardiac ventricular action potential:
642 model formulation and experimental validation. *PLoS Comput Biol* 7(5):e1002061.
- 643 37. Felix MA & Barkoulas M (2015) Pervasive robustness in biological systems. *Nat Rev Genet* 16(8):483-496.
- 644 38. Sandor V, *et al.* (2002) Phase I trial of the histone deacetylase inhibitor, depsipeptide (FR901228, NSC 630176), in patients
645 with refractory neoplasms. *Clin Cancer Res* 8(3):718-728.
- 646 39. Seki M, *et al.* (2016) Class I Histone Deacetylase Inhibition for the Treatment of Sustained Atrial Fibrillation. *J Pharmacol*
647 *Exp Ther.*
- 648 40. Baumgartner D, *et al.* (2007) Prolonged QTc intervals and decreased left ventricular contractility in patients with propionic
649 acidemia. *J Pediatr* 150(2):192-197, 197 e191.
- 650 41. Lucke T, *et al.* (2004) Propionic acidemia: unusual course with late onset and fatal outcome. *Metabolism* 53(6):809-810.
- 651 42. Jameson E & Walter J (2008) Cardiac arrest secondary to long QT(C) in a child with propionic acidemia. *Pediatr Cardiol*
652 29(5):969-970.
- 653 43. Tong L (2013) Structure and function of biotin-dependent carboxylases. *Cell Mol Life Sci* 70(5):863-891.
- 654 44. Sharp AJ, Cheng Z, & Eichler EE (2006) Structural variation of the human genome. *Annu Rev Genomics Hum Genet* 7:407-
655 442.
- 656 45. Giudicessi JR & Ackerman MJ (2013) Determinants of incomplete penetrance and variable expressivity in heritable cardiac
657 arrhythmia syndromes. *Transl Res* 161(1):1-14.
- 658 46. Cordeddu V, *et al.* (2009) Mutation of SHOC2 promotes aberrant protein N-myristoylation and causes Noonan-like
659 syndrome with loose anagen hair. *Nat Genet* 41(9):1022-1026.